LINC01137 involvement in pancreatic cancer stemness via the miR-7155-5p/KLF12/AKT axis

Chenghong Peng (chhpeng@yeah.net)
Ruijin Hospital, Shanghai Jiaotong University School of Medicine

Kexian Li
Ruijin Hospital, Shanghai Jiaotong University School of Medicine

Zengyu Feng
Ruijin Hospital, Shanghai Jiaotong University School of Medicine

Kai Qin
Ruijin Hospital, Shanghai Jiaotong University School of Medicine

Yang Ma
Ruijin Hospital, Shanghai Jiaotong University School of Medicine

Shiwei Zhao
Ruijin Hospital, Shanghai Jiaotong University School of Medicine

Peng Chen
Ruijin Hospital, Shanghai Jiaotong University School of Medicine

Jiewei Lin
Ruijin Hospital, Shanghai Jiaotong University School of Medicine

Yongsheng Jiang
Ruijin Hospital, Shanghai Jiaotong University School of Medicine

Lijie Han
Ruijin Hospital, Shanghai Jiaotong University School of Medicine

Yizhi Cao
Ruijin Hospital, Shanghai Jiaotong University School of Medicine

Jiaxin Luo
Ruijin Hospital, Shanghai Jiaotong University School of Medicine

Minmin Shi
Ruijin Hospital, Shanghai Jiaotong University School of Medicine

Hao Chen
Ruijin Hospital, Shanghai Jiaotong University School of Medicine

Jiancheng Wang
Ruijin Hospital, Shanghai Jiaotong University School of Medicine

Lingxi Jiang
Ruijin Hospital, Shanghai Jiaotong University School of Medicine

Research Article

Keywords: CSC, Biomarker, Stemness, Chemoresistance, KLF12, LINC01137, Has-miR-7155-5p

Posted Date: April 8th, 2022

DOI: https://doi.org/10.21203/rs.3.rs-1516835/v1

Abstract

Pancreatic cancer, which most commonly refers to pancreatic ductal adenocarcinoma (PDAC), is one of the most malignant tumors, with a 5-year survival rate of about 4%. Pancreatic cancer stem cells play pivotal roles in chemoresistance and recurrence. Long non-coding RNAs (lncRNAs) have been identified as key regulators of the biological progression of various cancers. Recently, lncRNAs were found to be associated with cancer stem cells, which are related to chemoresistance. LINC01137 has been reported as an oncogene in oral squamous cell carcinoma. However, its function and underlying mechanisms in pancreatic cancer remain unclear. Online datasets were used to screen for cancer stem cell-associated lncRNAs and to confirm the relationship between LINC01137 and stem genes. Quantitative real-time PCR was performed to detect RNA expression. In situ hybridization and nucleocytoplasmic separation were used to determine subcellular location. Direct binding of LINC01137 to miR-7155-5p was verified using a dual-luciferase reporter assay. LINC01137 was upregulated in pancreatic cancer tissues and cell lines. Its high expression correlated with advanced pathological stages and poor prognosis. Induction of LINC01137 expression boosted pancreatic cancer stemness, chemoresistance, and proliferation. Mechanistically, LINC01137 exerted its biological function by binding to miR-7155-5p to activate the KLF12/PI3K/AKT pathway. KLF12 also promoted LINC01137 expression. LINC01137 and KLF12 were involved in promoting PDAC tumorigenesis. Our results suggested that LINC01137 functions as an oncogene in pancreatic cancer and identified its post-transcriptional regulatory mechanisms, which may contribute to targeted therapy for pancreatic cancer.

Introduction

PDAC is the most common type of pancreatic malignant cancer (accounting for almost 85% of cases) (Vincent *et al.*,2011), and it remains an urgent worldwide healthcare problem. In America, it is the fourth leading cause of cancer death regardless of sex, also ranking 7th in China and 5th in males and 4th in females in the US Hispanic/Latino population, respectively (Chen *et al.*,2016; Miller *et al.*,2021; Siegel *et al.*,2021). Surgery is the only way to prolong PDAC patient survival. Owing to early diagnosis and emerging neoadjuvant therapy, an increasing number of patients can undergo surgery and show longer survival times (Cloyd *et al.*,2017; Murphy *et al.*,2018). Unfortunately, cancer recurrence and chemoresistance pose severe challenges for patients after pancreatectomy. Avoiding chemoresistance and recurrence has become a difficult challenge.

Cancer stem cells (CSCs) are a cluster of cancer tissues characterized by self-renewal and self-differentiation. CSCs induce heterogeneity in cancer (Reya *et al.*,2001). CSCs play a critical role in many biological processes involved in tumorigenesis (Batlle & Clevers,2017). Recent research has shown that although CSCs are not very abundant in cancer tissue, they contribute to recurrence and chemoresistance (Chen *et al.*,2012; Martins-Neves *et al.*,2016; Yang *et al.*,2020). Targeting CSCs could provide more opportunities to treat cancer. Except CSCs, non-stem cancer cells also sometimes show stem-cell-like phenotypes, described as gain of ‘stemness’ (Jopling *et al.*,2011). After gaining ‘stemness’,

cancer cells become more resistant to chemotherapy and recur more easily. Therefore, studying how cancer cells gain ‘stemness’ and maintain this phenotype can provide more targets to treat PDAC.

LINC01137, a 1443 bp mRNA, is an lncRNA located in 1p34.3. in oral squamous cell carcinoma, which positively promotes cancer development (Du *et al.*,2021). Bioinformatics analysis indicated that LINC01137 is associated with ferroptosis, autophagy, and redox in lung adenocarcinoma (Liu & Yang,2021; Ren *et al.*,2021; Yao *et al.*,2021) and indicated poor outcomes in high-grade serous ovarian cancer (Nakamura *et al.*,2022). Its biological function in pancreatic cancer is still unknown, and bioinformatics analysis has indicated that LINC01137 correlates with CSCs. Therefore, we designed experiments to determine the role of LINC01137 in PDAC and its clinical value.

Materials And Methods

Human cell lines and tissues

Five pancreatic cancer cell lines (AsPC-1, BxPC-3, CFPAC-1, Panc-1, and Pau8988) and human pancreatic ductal epithelial (HPNE) cells were purchased from the Cell Repository, Chinese Academy of Sciences (Shanghai, China). In addition, 293T cells were obtained from Shanghai Institute of Hematology. Panc-1, Patu8988, HPNE, and 293T cells were cultured in DMEM. AsPC-1 and BxPC-3 cells were grown in RPMI-1640. CFPAC-1 cells were grown in Iscove's modified Dulbecco's medium. All media contained 10% inactivated FBS (Gibco, Carlsbad, CA, USA), 1 × 105 U/L penicillin, and 100 mg/L streptomycin (Gibco). Cells were cultured in a humidified atmosphere containing 5% CO_2 at 37 °C. Seventy-two pairs of pancreatic cancer tissues and adjacent normal pancreatic tissues were collected at Ruijin Hospital affiliated with the Shanghai Jiaotong University School of Medicine (Shanghai, China). All 72 cancer samples were histologically identified as adenocarcinoma. All tissue samples were snap-frozen in liquid nitrogen and stored at -80 °C until use. All enrolled patients met the following criteria: (1) pathological diagnosis of pancreatic cancer, (2) complete clinicopathological and follow-up data, and (3) no preoperative chemotherapy. Written informed consent was obtained from all patients, and the study protocol was approved by the ethics committee of Ruijin Hospital.

RNA extraction and quantitative real-time PCR (qRT-PCR)

TRIzol reagent (Invitrogen, Carlsbad, CA) was used to extract total RNA, according to the manufacturer’s instructions. Cytoplasmic and nuclear RNA was extracted using the PARIS kit (Invitrogen). RNA samples were analyzed using NanoPhotomentN120(IMPLEN, Germany) to detect the concentrations and values of A260/A280 and A260/A230. CDNA was synthesized from 1 μg RNA using the Evo M-MLV RT Kit with the gDNA Clean for qPCR II kit (Accurate Biology, Hunan, China), according to the manufacturer’s instructions. QRT-PCR assays of mRNA expression levels were performed using SYBR® Green Premix Pro Taq HS qPCR Kit II (Accurate Biology, Hunan, China) on qTOWER^3 84G (Analytik Jena AG, Jena, Germany)

according to the manufacturer's instructions. The housekeeping genes U6 and glycerinaldehyde-3-phosphat-dehydrogenase (GAPDH) were used as reference genes. Primer sequences are listed in Table 1.

Western blot analysis

Cells were lysed in RIPA buffer (Beyotime, Shanghai, China) supplemented with a protease inhibitor cocktail (MCN Biotech, Suzhou, China), loaded, and separated on a 10% SDS-PAGE gel (EpiZyme, Shanghai, China). The samples were transferred onto polyvinylidene fluoride membranes and incubated with the following primary antibodies: anti-KLF12, anti-Cyclin D3, anti-CDK4, anti-CD44, anti-Sox2, anti-NANOG, anti-ALD1H1, anti-Oct4, anti-p-pb, anti-p21, anti-p-AKT, anti-AKT, anti-GAPDH (Table 2). GAPDH was used as the controls.

Immunohistochemistry

Subcutaneous tumor tissues from nude mice were fixed in 4% paraformaldehyde, dehydrated, and embedded in paraffin. The antigens were retrieved, and nonspecific binding was blocked using 4% normal goat serum (Gibco). Subsequently, cell coverslips were incubated with anti-PCNA, anti-CD44, and anti-CD133 primary antibodies (Table 3), followed by incubation with HRP-conjugated goat anti-rabbit IgG antibodies (1:1000, Cell Signaling, MA, USA). Then, 3,3-diaminobenzidine chromogen substrate solution was used to visualize the results.

Cell transfection

For *in vitro* experiments, miR-7155-5p mimics, negative control (NC) mimics, miR-7155-5p inhibitor, and NC inhibitor were synthesized by Tsingke (Beijing, China). Two shRNA-GFP vectors with two shRNA sequences targeting the 3'-UTR of LINC01137 and a NC shRNA-GFP vector were synthesized by Bioegene (Shanghai, China). Full-length LINC01137 and KLF12 cDNA was synthesized and inserted into a lentiviral vector or plasmid (Bioegene, Shanghai, China). BxPC-3, CFPAC-1, and PANC-1 cells transduced with the lentivirus were treated with 2 μg/mL puromycin for 48 h to establish stable cell lines. All transfections were performed using Lipofectamine 3000 (Invitrogen). The cells were collected 48 h post-transfection. The miRNA mimics and inhibitor, shRNA, and NC sequences are listed in Table 4.

Sphere formation assay

Pancreatic CSC (PCSC) spheres were generated by culturing primary pancreatic cancer cells (2000-4,000 cells/ml) in ultra-low attachment plates (Corning) in FBS-free DMEM/F12 (Invitrogen) supplemented with B27 1:50 (Invitrogen), 20 ng/mL bFGF (PAN-Biotech), and 50 U/mL penicillin/streptomycin (Thermo Fisher Scientific). Seven days later, the spheres were harvested, trypsinized into single cells, and re-

cultured for subsequent assays. Seven days later, the spheres were measured, counted, and photographed under a Zeiss Axio Vert A1 microscope (Zeiss, Oberkochen, Germany).

Cell proliferation assay

A CCK-8 kit was purchased from Meilune Bio (Dalian, China). The cells were plated in 96-well plates and treated for 24 h. Then, the CCK-8 reagent was added to the cells for another 4 h. Absorbance was measured using a microplate reader at 450 nm. A BeyoClick™ EdU Cell Proliferation Kit with Alexa Fluor 555 was purchased from Beyotime (Shanghai, China). The cells were plated in 12-well plates, cultured for 24 h, and then fixed using 4% paraformaldehyde and stained with DAPI after incubation with 50 mM EdU solution for 2 h. EdU-labeled cells were photographed under a Zeiss Axio Vert A1 microscope (Zeiss, Oberkochen, Germany).

Colony formation assay

The cells (1000-2000 cells/well) were seeded into 6-well plates and incubated with complete medium at 37 °C for 2–3 weeks. Then, the cells were fixed with 4% paraformaldehyde and stained with 2% crystal violet. Images were obtained, and the number of colonies was counted.

Flow cytometry (FCM)

Apoptosis rates were determined using FCM after staining with Annexin-V-7AAD and APC. The Annexin-V-7AAD and APC Apoptosis Detection Kit was purchased from BioLegend (San Diego, CA). The cells were plated in 6-well plates and treated as described in the Results section. Then, the cells were harvested, washed twice, resuspended in binding buffer, and stained with Annexin-V-7AAD and APC solution for 15 min at room temperature. Finally, the samples were subjected to FCM. After seeding in 6-well plates for 48 h, the cells were washed three times with cold PBS. Then, the supernatant was discarded via centrifugation, and the cells were resuspended at 1×10^6 cells/ml in 75% ethanol. After fixation at 4 ℃ for 8 h, cold ethanol was discarded via centrifugation, and the cells were washed with PBS twice. After removal of the supernatant, the cells were stained with 300 μl propidium iodide (Sigma, St. Louis, MO) for 30 min at 37 ℃ in a dark environment. CytoFLEX 5 (Beckman Coulter, Fullerton, CA) was used to record red fluorescence at an excitation wavelength of 488 nm to analyze the cell cycle. CD44 and CD133 antibodies were purchased from BioLegend (San Diego, CA) and used according to the manufacturer's protocol. CytoFLEX 5 (Beckman Coulter, Fullerton, CA) was applied to record APC-Cy7 and PE panel signals to analyze CD44 and CD133 status.

RNA fluorescence *in situ* hybridization (FISH)

Cy3-labeled LINC01137 probes were purchased from RiboBio (Guangzhou, China). BxPC-3, CFPAC-1, and Panc-1 cells were fixed with 4% formaldehyde and permeabilized with 0.5% TritonX-100. The cells were then hybridized with Cy3-labeled probes. The nuclei were stained with DAPI. Images were acquired using a Zeiss LSM900 (Zeiss, Oberkochen, Germany).

Luciferase reporter assays

Wild-type (WT) and mutant (MUT) 3-UTRs of LINC01137 and KLF12 reporter plasmids were constructed through BioGene (Shanghai, China). Then, 293T cells were co-transfected with luciferase constructs and miR-7155-5p mimics, according to the manufacturer's protocol. After transfection for 48 h, luciferase activity was measured using a dual-luciferase reporter assay kit (Vazyme). Each experiment was conducted in triplicates.

In vivo tumorigenicity model

Animal experiments were conducted with the approval of the Animal Ethics Committee of Ruijin Hospital, affiliated with the Shanghai Jiaotong University School of Medicine (Shanghai, China). The pancreatic cancer cells were digested and suspended in cold PBS at a density of 10^8 cells/ml. Approximately 100 μl of the cell suspension containing 10^7 cells was injected subcutaneously into 4–5-week-old male BALB/c nude mice on the right and left sides of the armpit. After almost a month, the tumors were harvested and analyzed.

In vivo limiting dilution assays

Pancreatic cancer cells were digested and suspended in cold PBS at a density of 10^7–10^4 cells/ml at four concentrations. Approximately 100 μl of cell suspension, containing 10^6–10^3 cells, was injected subcutaneously into 4–5-week-old male BALB/c nude mice on the right and left sides of the armpit. After almost a month, the tumors were harvested and analyzed. CSC frequency assay was followed by previous research(Hu & Smyth,2009).

Bioinformatic analysis

The gene expression profiles and related clinical data of patients were retrieved and downloaded from The Cancer Genome Atlas (TCGA) database. Dataset GSE51971 was retrieved and downloaded from Gene Expression Omnibus (GEO) database. Dataset MTAB6690 was downloaded from ArrayExpress database. The Box plot and prognosis analysis about data from TCGA were plotted by GEPIA (http://gepia.cancer-pku.cn/index.html). The heatmap was plotted by http://www.bioinformatics.com.cn, a free online platform for data analysis and visualization. The potential subcellular localization of

LINC01137 was predicted on lncLocator(Lin *et al.*,2021b). The microRNAs that are interacting with LINC01137 were predicted using DIANA(Paraskevopoulou *et al.*,2016), miRDB(Chen & Wang,2020), and LNCSNP2 (http://bioinfo.life.hust.edu.cn/lncRNASNP#!/) datasets. The mRNAs that bind to miR-7155-5p were predicted through miRDB(Chen & Wang,2020), miRWalk(Sticht *et al.*,2018), miRPathDB(Kehl *et al.*,2020), and TargetScan (http://www.targetscan.org/vert_71/) datasets.

Statistical analysis

Statistical analyses were performed using SPSS 20.0 and GraphPad Prism 8.0. Experiments were repeated independently at least three times, and the results are presented as the means ± standard deviation (SD). One-way analysis of variance, Student's t-test, and chi-squared test were used to analyze the differences between different groups. Survival curves were analyzed using the Kaplan–Meier method, and log-rank tests were used to evaluate differences between the groups. Statistical significance was set at $p < 0.05$.

Results

Higher LINC01137 expression in PCSCs was associated with poor outcome

Data from GSE51971 dataset were used to identify different long intergenic lncRNAs in PCSC-like and non-PCSC-like cells. There were 30 upregulated long intergenic lncRNAs in PCSC-like cells (Fig. 1a). Correlation between these genes and stem cell markers showed that LINC01137 was highly associated with CD133 and CD44 in TCGA and MTAB6690 (Fig. 1b). In TCGA dataset, LINC01137 expression was higher in tumor tissues than in the associated normal tissues (Fig. 1c). Meanwhile, higher LINC01137 expression was associated with a worse overall outcome and shorter disease-free survival time (Fig. 1d-e). In addition, LINC01137 expression increased with pancreatic grade increase (Fig. 1f). In our center, LINC01137 expression was higher in tumor tissues than in paired normal tissues, and higher LINC01137 expression associated with a worse overall outcome (Fig. 1g-h). LINC01137 appeared to be a signature of cancer stemness and seemed able to predict the outcome of PDAC. Therefore, we used LINC01137 and studied it further. The expression of LINC01137 was determined in five pancreatic cancer cell lines (AsPC-1, BxPC-3, CFPAC-1, Panc-1, and Patu8988) and in HPNE cells. LINC01137 expression was higher in pancreatic cancer cell lines than in HPNE cells (Fig. 1i). The CFPAC-1 and Panc-1 cell lines were used for LINC01137 knockdown (Fig. 1j), and the BxPC-3 and Panc-1 cell lines were used to overexpress LINC01137 (Fig. S1a).

LINC01137 promoted PDAC stemness and gemcitabine chemoresistance

Since LINC01137 was related to CSCs, the extent of stemness in CFPAC-1 and Panc-1 cell lines was first examined *in vitro*. As expected, when LINC01137 expression decreased, sphere cells manifested lower sphere numbers and shorter sphere diameters. This phenomenon was observed in both CFPAC-1 and Panc-1 cell lines (Fig. 2a-b). Second, CD44 and CD133 expression was detected using FCM. Compared with the control group, the sh-LINC01137 group showed fewer $CD133^+$ cells in the CFPAC-1 cell line and fewer CD44+ cells in the Panc-1 cell line under normal culture conditions (Fig. 2c-d, Fig. S2a). LINC01137 overexpression increased CD44+ expression in Panc-1 cells (Fig. S2b). In addition, stemness-related protein (such as CD44, NANOG, and ALD1H1) expression was impaired by LINC01137 knockdown (Fig. 2e). Limiting dilution assays built a model to estimate CSC frequency *in vivo*. Only the control group grew when the number of injected cells was less than 10^4 in the CFPAC-1 cell line, while the same phenomenon was detected in the Panc-1 cell line when less than 10^5 cells were injected (Fig. 2h). LINC01137 knockdown led to more than 60% reduction in CSC frequency *in vivo* (Fig. S2c). LINC01137 knockdown reduced the expression of stemness marker genes CD44 and CD133 *in vivo* (Fig. 2i). Taken together, LINC01137 promoted stemness in pancreatic cancer cells. Many studies have found that CSCs contribute to chemoresistance; therefore, we examined whether LINC01137 promotes PDAC resistance to gemcitabine, which is a first-line chemotherapeutic drug in the clinic. *In vitro*, after LINC01137 knockdown in the CFPAC-1 and Panc-1 cell lines, the IC_{50} of gemcitabine decreased (Fig. 2f), and more cells underwent apoptosis (Fig. 2g). LINC01137 overexpression increased the IC_{50} of gemcitabine in BxPC3 (Fig. S2d). LINC01137 was upregulated in gemcitabine-resistant cells, compared with their parent cells (Fig. S2e). Thus, LINC01137 decreased PDAC cell sensitivity to gemcitabine. Taken together, these results suggest that LINC01137 promotes PDAC stemness and chemoresistance.

LINC01137 promoted PDAC proliferation and cell cycle

Next, we investigated the effect of LINC01137 on cell proliferation. *In vitro*, silencing LINC01137 markedly slowed the growth of both PDAC cell lines (CFPAC-1 and Panc-1), as determined using the CCK-8 (Fig. 3a) and colony formation (Fig. 3b) assays. LINC01137 overexpression accelerated PDAC cell growth (Fig. S3a-b). Consistently, the EdU assay indicated that the knockdown group had fewer EdU-positive cells than the control group (Fig. 3c). Meanwhile, LINC01137 overexpression increased EdU-positive cells (Fig. S3c). Consistent with the *in vitro* findings, tumors with LINC01137 knockdown grew slowly and weighed less (Fig. 3f). Furthermore, tumors with LINC01137 knockdown had fewer PCNA-positive cells than those without LINC01137 knockdown (Fig. 3g), indicating that LINC01137 knockdown impeded cell proliferation *in vivo*. FCM was performed to determine whether LINC01137 regulated the cell cycle. More LINC01137-silenced cells were arrested in the G1 phase, compared with control cells (Fig. S3d). To further investigate whether LINC01137 plays a critical role in the G1/S checkpoint, PDAC cells (CFPAC-1 and Panc-1) were synchronized in the G0/1 phase via serum starvation (Fig. S3e). Re-treated with medium with FBS 12 h after starvation, more cells shifted into the G2/S phase, compared with knockdown group (Fig. 3d). The expression levels of key cell cycle proteins were also decreased in cells with lower

LINC01137 expression levels (Fig. 3e). Taken together, these results indicated that LINC01137 accelerates PDAC proliferation by prolonging the cell cycle period.

LINC01137 as a competing endogenous RNA (ceRNA) targeted miR-7155-5p to promote PDAC tumorigenesis

We used lncLocator to predict the subcellular localization of LINC01137. It predicted that LINC01137 mostly located in the cytoplasm (Fig. 4a). FISH and nucleocytoplasmic separation assays were performed to determine the subcellular localization of LINC01137. The results showed that LINC01137 was present in the cytoplasm (Fig. 4b-c). This finding suggests that LINC01137 exerts its biological function by acting as a ceRNA. Three public datasets (DIANA, miRDB, and LNCSNP2) were used to predict miRNA candidates. Three miRNAs (miR-765, miR-4664-5p, and miR-7155-5p) were predicted to interact with LINC01137 in the three datasets (Fig. 4d). The expression of these miRNAs in CFPAC-1 and Panc-1-knockdown cell lines was evaluated using qRT-PCR. In both cell lines, the expression level of miR-7155-5p increased in LINC01137-silenced cells (Fig. 4e). Therefore, miR-7155-5p was selected for further experiments. The negative correlation between LINC01137 and miR-7155-5p was significant in our center (Fig. 4f). A dual-luciferase reporter assay was performed to verify the interaction between LINC01137 and miR-7155-5p. WT and MUT LINC01137 3’-UTRs were designed by Bioegene (Shanghai, China) (Fig. 4g). As expected, there was a significant reduction in luciferase activity after co-transfection of miR-7155-5p mimics and a WT LINC01137 reporter vector, but this reduction was not observed after the transfection of MUT LINC01137 reporter vectors (Fig. 4h), suggesting an interaction between LINC01137 and miR-7155-5p. Sh-LINC01137#2 group was used for following research. The expression of miR-7155-5p after transfection with the inhibitor was detected using qRT-PCR (Fig. 5a). For tumor proliferation, reducing miR-7155-5p expression boosted PDAC duplication speed (Fig. 5b-c). After infection with the miR-7155-5p inhibitor, the CD133/CD44-negetive cell ratio ratio decreased and stemness-related protein expression increased (Fig. 5f-g). Regarding chemoresistance, after downgrading miR-7155-5p expression, the IC_{50} of gemcitabine increased in both CFPAC-1 and Panc-1 Sh-LINC01137#2 cell lines, while less cell apoptosis was observed with gemcitabine for 48 h (Fig. 5e). Based on this evidence, we concluded that LINC01137 promotes PDAC malignancy through miR-7155-5p.

LINC01137 regulated KLF12 through miR-7155-5p

RNA sequencing and public datasets were used to predict the downstream mRNAs for further research. Four datasets (miRDB, miRWalk, miRPathDB, and TargetScan) were used to predict the mRNAs, which miR-7155-5p may interact with, and 496 mRNAs were found. RNA sequencing data were used to screen for significant mRNAs, and 13 mRNAs were found (Fig. 6a). Among these mRNAs, KLF12 was reported associated with CSCs(Bialkowska *et al.*,2017; He *et al.*,2019b). Its expression in the CFPAC-1 and Panc-1 cell line was tested using western blotting analysis. KLF12 expression was downregulated after

LINC01137 knockdown (Fig. S4a). The negative correlation between miR-7155-5p and KLF12 and positive correlation between LINC01137 and KLF12 were significant in our center (Fig. 6b). A dual-luciferase reporter assay was performed to verify the interaction between miR-7155-5p and KLF12. Luciferase activity was decreased by co-transfecting miR-7155-5p mimics and a WT KLF12 3'-UTR reporter vectors, but this reduction was not observed after co-transfecting miR-7155-5p mimics and MUT KLF12 3'-UTR reporter vectors (Fig. 6c). After infection with miR-7155-5p mimics, KLF12 expression decreased in the CFPAC-1 and Panc-1 cell lines (Fig. S4b). Taken together, these results suggested that miR-7155-5p interacts with KLF12. A KLF12 rescue experiment was performed. KLF12 overexpression effect was verified through qRT-PCR and western blotting analysis (Fig. 6d). KLF12 overexpression boosted cell proliferation capacity, as shown by the CCK-8 and colony formation assays (Fig. 6e-f). For the stemness phenotype, the CD133/CD44-negetive cell ratio was decreased, and stemness-related protein expression was also enhanced (Fig. 6i-j). For chemoresistance assays, fewer cells underwent apoptosis, and the IC_{50} slightly increased after transfection with the KLF12 vector (Fig. 6g-h). This indicated that LINC01137 may regulate KLF12 to promote PDAC tumorigenesis.

LINC01137 participated in the PI3K/Akt pathway to promote PDAC tumorigenesis through regulating KLF12

Previous studies have indicated that KLF12 participates in the PI3K/Akt pathway to regulate biological activities (He *et al.*,2019c). Our RNA sequencing results also confirmed that LINC01137 could regulate the PI3K/Akt pathway (Fig. 7a). Western blotting results indicated that, compared with the control group, the LINC01137-knockdown group had a lower PI3K/Akt-related protein expression grade. With miR-7155-5p downregulation and KLF12 overexpression, this decreasing trend was reversed (Fig. 7b). Furthermore, Jasper (https://jaspar.genereg.net/) was used to predict the molecules that KLF12 regulates. Interestingly, LINC01137 was found to be a potent molecule regulated by KLF12 (Fig. 7c). After KLF12 overexpression, LINC01137 expression increased simultaneously in the BxPC-3 and Panc-1 cell lines (Fig. 7d). Thus, LINC01137 and KLF12 may form a loop that facilitates PDAC tumorigenesis (Fig. 7e).

Discussion

Pancreatic cancer, especially PDAC, is the most malignant gastrointestinal tumor and is characterized by late diagnosis, easy recurrence, metastasis, and chemoresistance (McGuigan *et al.*,2018). Although neoadjuvant chemotherapy has been utilized to provide more patients with the chance to undergo surgery, the 5-survival rate is still low (Heinrich & Lang,2017). Chemoresistance has become a difficult problem to overcome. A recent study showed that PCSCs are associated with chemoresistance, and focusing on them could provide more therapeutic targets (Cazet *et al.*,2018; Wang *et al.*,2018).

LncRNAs participate in many normal and malignant biological processes. It has been reported that lncRNAs are associated with tumor stemness and chemoresistance (He *et al.*,2019a; Ren *et al.*,2018). Furthermore, lncRNAs have many crucial functions in PDAC and are valuable for early diagnosis and

long-term prognosis. For instance, FLVCR1-AS1 plays a tumor-suppressive role in PDAC by sponging miR-513c-5p or miR-514b-5p to inhibit proliferation, cell cycle, and migration (Lin *et al.*,2021a), whereas LINC00261 inhibits c-Myc-mediated aerobic glycolysis in PDCA by sponging miR-222-3p and downgrading IGF2BP1 (Zhai *et al.*,2021). LINC01137 is predicted to be associated with ferroptosis, autophagy, and redox reactions(Liu & Yang,2021; Ren *et al.*,2021; Yao *et al.*,2021). In oral squamous cell carcinoma(Du *et al.*,2021). LINC01137 promotes cancer development (Du *et al.*,2021). However, the biological function of LINC01137 in pancreatic cancer remains unclear. Expression was analyzed using TCGA and Ruijin cohorts, and we found that LINC01137 expression was significantly increased in tumor tissues, compared with the paired normal tissues. LINC01137 was associated with poor outcomes, as indicated by survival analysis, increasing with clinical stage. Thus, LINC01137 is a potential biomarker for PDAC. Functional *in vitro* and *in vivo* experiments demonstrated that LINC01137 maintains tumor stemness and chemoresistance and promotes PDAC tumorigenesis.

Considering that the function of lncRNAs depends on their location (Bridges *et al.*,2021), we used FISH and subcellular fractionation assays to determine the distribution of LINC01137. The results suggested that LINC01137 is mostly located in the cytoplasm. Cytoplasmic lncRNAs are widely recognized as ceRNA-binding miRNAs. We used three datasets to predict miRNAs that bind to LINC01137. Has-miR-7155-5p was selected for further analysis based on the qRT-PCR results. We determined the binding site in the LINC01137 3’-UTR with miR-7155-5p and confirmed the interaction via dual-luciferase reporter assays.

Rescue experiments were performed using LINC01137-knockdown cells. We found that after reducing miR-7155-5p expression, more cancer cells maintained their stemness, and they were less sensitive to gemcitabine and showed accelerated proliferation. This suggested that LINC01137 acts as a ceRNA-binding miR-7155-5p to promote PDAC tumorigenesis.

Proteins are terminal molecules with biological functions. A ceRNA hypothesis states that miRNA is bound by lncRNA, so it cannot bind mRNA, resulting in mRNA translation into protein(Salmena *et al.*,2011). We used four databases to predict the potential target mRNAs. We combined database information with RNA sequencing results to select KLF12 as the downstream mRNA. KLF12, also known as Krüppel-like factor 12, is a member of the Krüppel-like factor family, whose members function as transcriptional regulators in a multitude of cancer-relevant processes (Bialkowska *et al.*,2017; Tetreault *et al.*,2013). KLF12 facilitates many biological processes in multiple cancers, including pancreatic cancer (Chen *et al.*,2021; He *et al.*,2019b; Hou & Li,2020; Xu *et al.*,2021; Xun *et al.*,2019). We determined the binding site in the KLF12 3’-UTR with miR-7155-5p and confirmed the interaction via dual-luciferase reporter assays. After rescuing KLF12 expression in LINC01137-knockdown cells, stemness, chemoresistance, and proliferation were enhanced. Altogether, LINC01137 mediates KLF12 expression by sponging miR-7155-5p as a ceRNA.

However, our study had some limitations. The stemness phenotype was a PCSC derivative, and we have not studied the role of LINC01137 in PCSCs. Furthermore, the relationship between stemness and

chemoresistance under LINC01137 is still unclear and requires further discussion. The mechanism, by which KLF12 regulates the PI3K/AKT pathway and LINC01137 requires further investigation.

Declarations

Availability of data and material

The authors declare that the data supporting the findings of this study are available within the paper.

Acknowledgements

The authors thank Xiaomei Tang, Jia Liu and Xiongyan Wu for experimental assistance.

Author Contribution

Kexian Li and Zengyu Feng carried out in vivo and in vitro experiments, and manuscript preparation. Kexian Li and Kai Qin carried out statistical analysis, Yang Ma and Shiwei Zhao carried out qRT-PCR analysis, Peng Chen and Jiewei Lin carried out bioinformatics analysis, Yongsheng Jiang, Lijie Han, Yizhi Cao and Jiaxin Luo carried out IHC, Minmin Shi and Hao Chen carried out clinical information about patients of PDAC sample, Jiancheng Wang, Lingxi Jiang and Chenghong Peng designed, supervised and interpreted the study.

Funding sources

This work was supported by grants from the National Natural Science Foundation of China (82173226).

Disclosure of conflicts of interest

The authors declare no potential conflicts of interest.

Ethics Statement and Consent to Participate

Studies using human tissues were reviewed and approved by the Committees for Ethical Review of Research involving Human Subjects of Ruijin Hospital affiliated with Shanghai Jiaotong University School of Medicine. The study was performed in accordance with the Declaration of Helsinki.

Consent for Publication

The study was undertaken with the patient’s consent.

Code Availability

All bioinformatic analysis use online tools that were described in method.

References

1. Batlle E., and Clevers H. Cancer stem cells revisited. *Nat Med*. (2017); 23: 1124-1134.doi:10.1038/nm.4409
2. Bialkowska AB, Yang VW., and Mallipattu SK. Krüppel-like factors in mammalian stem cells and development. *Development*. (2017); 144: 737-754.doi:10.1242/dev.145441
3. Bridges MC, Daulagala AC., and Kourtidis A. LNCcation: lncRNA localization and function. *J Cell Biol*. (2021); 220.doi:10.1083/jcb.202009045
4. Cazet AS, Hui MN, Elsworth BL, Wu SZ, Roden D, Chan CL, et al. Targeting stromal remodeling and cancer stem cell plasticity overcomes chemoresistance in triple negative breast cancer. *Nat Commun*. (2018); 9: 2897.doi:10.1038/s41467-018-05220-6
5. Chen H, Wu C, Luo L, Wang Y., and Peng F. circ_0000467 promotes the proliferation, metastasis, and angiogenesis in colorectal cancer cells through regulating KLF12 expression by sponging miR-4766-5p. *Open Med (Wars)*. (2021); 16: 1415-1427.doi:10.1515/med-2021-0358
6. Chen J, Li Y, Yu T-S, McKay RM, Burns DK, Kernie SG, et al. A restricted cell population propagates glioblastoma growth after chemotherapy. *Nature*. (2012); 488: 522-526.doi:10.1038/nature11287
7. Chen W, Zheng R, Baade PD, Zhang S, Zeng H, Bray F, et al. Cancer statistics in China, 2015. *CA Cancer J Clin*. (2016); 66: 115-32.doi:10.3322/caac.21338
8. Chen Y., and Wang X. miRDB: an online database for prediction of functional microRNA targets. *Nucleic Acids Res*. (2020); 48: D127-d131.doi:10.1093/nar/gkz757
9. Cloyd JM, Katz MH, Prakash L, Varadhachary GR, Wolff RA, Shroff RT, et al. Preoperative Therapy and Pancreatoduodenectomy for Pancreatic Ductal Adenocarcinoma: a 25-Year Single-Institution Experience. *J Gastrointest Surg*. (2017); 21: 164-174.doi:10.1007/s11605-016-3265-1
10. Du Y, Yang H, Li Y, Guo W, Zhang Y, Shen H, et al. Long non-coding RNA LINC01137 contributes to oral squamous cell carcinoma development and is negatively regulated by miR-22-3p. *Cellular Oncology*. (2021); 44: 595-609.doi:10.1007/s13402-021-00586-0
11. He W, Liang B, Wang C, Li S, Zhao Y, Huang Q, et al. MSC-regulated lncRNA MACC1-AS1 promotes stemness and chemoresistance through fatty acid oxidation in gastric cancer. *Oncogene*. (2019a); 38: 4637-4654.doi:10.1038/s41388-019-0747-0
12. He Z, Guo X, Tian S, Zhu C, Chen S, Yu C, et al. MicroRNA-137 reduces stemness features of pancreatic cancer cells by targeting KLF12. *J Exp Clin Cancer Res*. (2019b); 38: 126.doi:10.1186/s13046-019-1105-3
13. He Z, Guo X, Tian S, Zhu C, Chen S, Yu C, et al. MicroRNA-137 reduces stemness features of pancreatic cancer cells by targeting KLF12. *Journal of Experimental & Clinical Cancer Research*. (2019c); 38: 126.doi:10.1186/s13046-019-1105-3
14. Heinrich S., and Lang H. Neoadjuvant Therapy of Pancreatic Cancer: Definitions and Benefits. *Int J Mol Sci*. (2017); 18.doi:10.3390/ijms18081622
15. Hou YS., and Li X. Circ_0005273 induces the aggravation of pancreatic cancer by targeting KLF12. *Eur Rev Med Pharmacol Sci*. (2020); 24: 11578-11586.doi:10.26355/eurrev_202011_23799

16. Hu Y., and Smyth GK. ELDA: extreme limiting dilution analysis for comparing depleted and enriched populations in stem cell and other assays. *J Immunol Methods*. (2009); 347: 70-8.doi:10.1016/j.jim.2009.06.008
17. Jopling C, Boue S., and Belmonte JCI. Dedifferentiation, transdifferentiation and reprogramming: three routes to regeneration. *Nature Reviews Molecular Cell Biology*. (2011); 12: 79-89.doi:10.1038/nrm3043
18. Kehl T, Kern F, Backes C, Fehlmann T, Stöckel D, Meese E, et al. miRPathDB 2.0: a novel release of the miRNA Pathway Dictionary Database. *Nucleic Acids Res*. (2020); 48: D142-d147.doi:10.1093/nar/gkz1022
19. Lin J, Zhai S, Zou S, Xu Z, Zhang J, Jiang L, et al. Positive feedback between lncRNA FLVCR1-AS1 and KLF10 may inhibit pancreatic cancer progression via the PTEN/AKT pathway. *J Exp Clin Cancer Res*. (2021a); 40: 316.doi:10.1186/s13046-021-02097-0
20. Lin Y, Pan X., and Shen HB. lncLocator 2.0: a cell-line-specific subcellular localization predictor for long non-coding RNAs with interpretable deep learning. *Bioinformatics*. (2021b).doi:10.1093/bioinformatics/btab127
21. Liu B., and Yang S. A Five Autophagy-Related Long Non-Coding RNA Prognostic Model for Patients with Lung Adenocarcinoma. *Int J Gen Med*. (2021); 14: 7145-7158.doi:10.2147/ijgm.S334601
22. Martins-Neves SR, Paiva-Oliveira DI, Wijers-Koster PM, Abrunhosa AJ, Fontes-Ribeiro C, Bovée JVMG, et al. Chemotherapy induces stemness in osteosarcoma cells through activation of Wnt/β-catenin signaling. *Cancer Lett*. (2016); 370: 286-295.doi:https://doi.org/10.1016/j.canlet.2015.11.013
23. McGuigan A, Kelly P, Turkington RC, Jones C, Coleman HG., and McCain RS. Pancreatic cancer: A review of clinical diagnosis, epidemiology, treatment and outcomes. *World J Gastroenterol*. (2018); 24: 4846-4861.doi:10.3748/wjg.v24.i43.4846
24. Miller KD, Ortiz AP, Pinheiro PS, Bandi P, Minihan A, Fuchs HE, et al. Cancer statistics for the US Hispanic/Latino population, 2021. *CA Cancer J Clin*. (2021); 71: 466-487.doi:10.3322/caac.21695
25. Murphy JE, Wo JY, Ryan DP, Jiang W, Yeap BY, Drapek LC, et al. Total Neoadjuvant Therapy With FOLFIRINOX Followed by Individualized Chemoradiotherapy for Borderline Resectable Pancreatic Adenocarcinoma: A Phase 2 Clinical Trial. *JAMA Oncol*. (2018); 4: 963-969.doi:10.1001/jamaoncol.2018.0329
26. Nakamura K, Reid BM, Chen A, Chen Z, Goode EL, Permuth JB, et al. Functional analysis of the 1p34.3 risk locus implicates GNL2 in high-grade serous ovarian cancer. *Am J Hum Genet*. (2022); 109: 116-135.doi:10.1016/j.ajhg.2021.11.020
27. Paraskevopoulou MD, Vlachos IS, Karagkouni D, Georgakilas G, Kanellos I, Vergoulis T, et al. DIANA-LncBase v2: indexing microRNA targets on non-coding transcripts. *Nucleic Acids Res*. (2016); 44: D231-8.doi:10.1093/nar/gkv1270
28. Ren J, Ding L, Zhang D, Shi G, Xu Q, Shen S, et al. Carcinoma-associated fibroblasts promote the stemness and chemoresistance of colorectal cancer by transferring exosomal lncRNA H19. *Theranostics*. (2018); 8: 3932-3948.doi:10.7150/thno.25541

29. Ren J, Wang A, Liu J., and Yuan Q. Identification and validation of a novel redox-related lncRNA prognostic signature in lung adenocarcinoma. *Bioengineered*. (2021); 12: 4331-4348.doi:10.1080/21655979.2021.1951522
30. Reya T, Morrison SJ, Clarke MF., and Weissman IL. Stem cells, cancer, and cancer stem cells. *Nature*. (2001); 414: 105-111.doi:10.1038/35102167
31. Salmena L, Poliseno L, Tay Y, Kats L., and Pandolfi PP. A ceRNA hypothesis: the Rosetta Stone of a hidden RNA language? *Cell*. (2011); 146: 353-8.doi:10.1016/j.cell.2011.07.014
32. Siegel RL, Miller KD, Fuchs HE., and Jemal A. Cancer Statistics, 2021. *CA Cancer J Clin*. (2021); 71: 7-33.doi:10.3322/caac.21654
33. Sticht C, De La Torre C, Parveen A., and Gretz N. miRWalk: An online resource for prediction of microRNA binding sites. *PLoS ONE*. (2018); 13: e0206239.doi:10.1371/journal.pone.0206239
34. Tetreault MP, Yang Y., and Katz JP. Krüppel-like factors in cancer. *Nat Rev Cancer*. (2013); 13: 701-13.doi:10.1038/nrc3582
35. Vincent A, Herman J, Schulick R, Hruban RH., and Goggins M. Pancreatic cancer. *Lancet*. (2011); 378: 607-20.doi:10.1016/s0140-6736(10)62307-0
36. Wang T, Fahrmann JF, Lee H, Li YJ, Tripathi SC, Yue C, et al. JAK/STAT3-Regulated Fatty Acid β-Oxidation Is Critical for Breast Cancer Stem Cell Self-Renewal and Chemoresistance. *Cell Metab*. (2018); 27: 136-150.e5.doi:10.1016/j.cmet.2017.11.001
37. Xu C, Shao Y, Liu J, Yao X, Quan F, Zhao Q, et al. Long non-coding RNA AGAP2-AS1 promotes proliferation and metastasis in papillary thyroid cancer by miR-628-5p/KLF12 axis. *J Bioenerg Biomembr*. (2021); 53: 235-245.doi:10.1007/s10863-021-09879-3
38. Xun J, Wang C, Yao J, Gao B., and Zhang L. Long Non-Coding RNA HOTAIR Modulates KLF12 to Regulate Gastric Cancer Progression via PI3K/ATK Signaling Pathway by Sponging miR-618. *Onco Targets Ther*. (2019); 12: 10323-10334.doi:10.2147/ott.S223957
39. Yang L, Shi P, Zhao G, Xu J, Peng W, Zhang J, et al. Targeting cancer stem cell pathways for cancer therapy. *Signal Transduct Target Ther*. (2020); 5: 8.doi:10.1038/s41392-020-0110-5
40. Yao J, Chen X, Liu X, Li R, Zhou X., and Qu Y. Characterization of a ferroptosis and iron-metabolism related lncRNA signature in lung adenocarcinoma. *Cancer Cell Int*. (2021); 21: 340.doi:10.1186/s12935-021-02027-2
41. Zhai S, Xu Z, Xie J, Zhang J, Wang X, Peng C, et al. Epigenetic silencing of LncRNA LINC00261 promotes c-myc-mediated aerobic glycolysis by regulating miR-222-3p/HIPK2/ERK axis and sequestering IGF2BP1. *Oncogene*. (2021); 40: 277-291.doi:10.1038/s41388-020-01525-3

Tables

Table 1

Primer sequence.

Primer	Sequence(5' to 3')
LINC01137-F	GTGATGCCACTCCCTAACCC
LINC01137-R	CCTTTGGCTTAGGGCATCCT
GAPDH-F	GGAGCGAGATCCCTCCAAAAT
GAPDH-R	GGCTGTTGTCATACTTCTCATGG
U6 RT Primer	CGCTTCACGAATTTGCGTGTCAT
U6-F	GCTTCGGCAGCACATATACTAAAAT
U6-R	CGCTTCACGAATTTGCGTGTCAT
hsa-miR-7155-5p-Rtprimer	GTCGTATCCAGTGCAGGGTCCGAGGTATTCGCACTGGATACGACGATGGC
hsa-miR-7155-5p-F	CGCGTCTGGGGTCTTGG
hsa-miR-7155-5p-R	AGTGCAGGGTCCGAGGTATT
hsa-miR-4664-5p-RTprimer	GTCGTATCCAGTGCAGGGTCCGAGGTATTCGCACTGGATACGACAACTTG
hsa-miR-4664-5p-F	TGGGGTGCCCACTCCG
hsa-miR-4664-5p-R	AGTGCAGGGTCCGAGGTATT
hsa-miR-765-RTprimer	GTCGTATCCAGTGCAGGGTCCGAGGTATTCGCACTGGATACGACCATCAC
hsa-miR-765-F	CGCGTGGAGGAGAAGGAAG
hsa-miR-765-R	AGTGCAGGGTCCGAGGTATT
KLF12-F	ATGTGATTTTGAGGGATGCAAC
KLF12-R	CAAATGATCTGACCGGGAAAAG

Table 2

Primary antibodies for western blotting.

Antibody	Company	Cat. No.	Species	Dilution
GAPDH	Proteintech	60004-1-Ig	Mouse	1:1000
p-AKT	Cell Signaling Technology	4060	Rabbit	1:2000
CD44	Proteintech	60224-1-Ig	Mouse	1:2000
Sox2	Cell Signaling Technology	3579	Rabbit	1:1000
Oct-4A	Cell Signaling Technology	2840	Rabbit	1:1000
p-Rb	Cell Signaling Technology	8516	Rabbit	1:1000
p21	Cell Signaling Technology	2947	Rabbit	1:1000
KLF12	Proteintech	13156-1-AP	Rabbit	1:1000
ALDH1A1	Cell Signaling Technology	54135	Rabbit	1:1000
NANOG	Cell Signaling Technology	4903	Rabbit	1:2000
Cyclin D3	Cell Signaling Technology	2936	Mouse	1:2000
CDK4	Cell Signaling Technology	12790	Rabbit	1:1000
AKT	Cell Signaling Technology	4685	Rabbit	1:1000

Table 3

Primary antibodies for IHC

Antibody	Company	Cat. No.	Species	Dilution
CD133	Proteintech	18470-1-AP	Rabbit	1:500
CD44	Proteintech	60224-1-Ig	Mouse	1:500
PCNA	Servicebio	GB11010	Rabbit	1:500

Table 4

MiRNA mimics and inhibitor, shRNA, and NC sequences.

Name	Nucleotide sequence (5' to 3')
hsa-miR-7155-5p inhibitor	GAUGGCCCAAGACCCCAGA
inhibitor NC	UCUACUCUUUCUAGGAGGUUGUGA
hsa-miR-7155-5p-mimics sense	UCUGGGGUCUUGGGCCAUC
hsa-miR-7155-5p-mimics antisense	UGGCCCAAGACCCCAGAUU
mimics NC sense	UCACAACCUCCUAGAAAGAGUAGA
mimics NC antisense	UCUACUCUUUCUAGGAGGUUGUGA
sh-LINC01137#1 sense	GGGTGAGAACCTACTTCTTCA
sh-LINC01137#1 antisense	TGAAGAAGTAGGTTCTCACCC
sh-LINC01137#2 sense	GCATCATGCATGTAACTTTCA
sh-LINC01137#2 antisense	TGAAAGTTACATGCATGATGC
sh-Control sense	TTCTCCGAACGTGTCACGT
sh-Control antisense	ACGTGACACGTTCGGAGAA

Figures

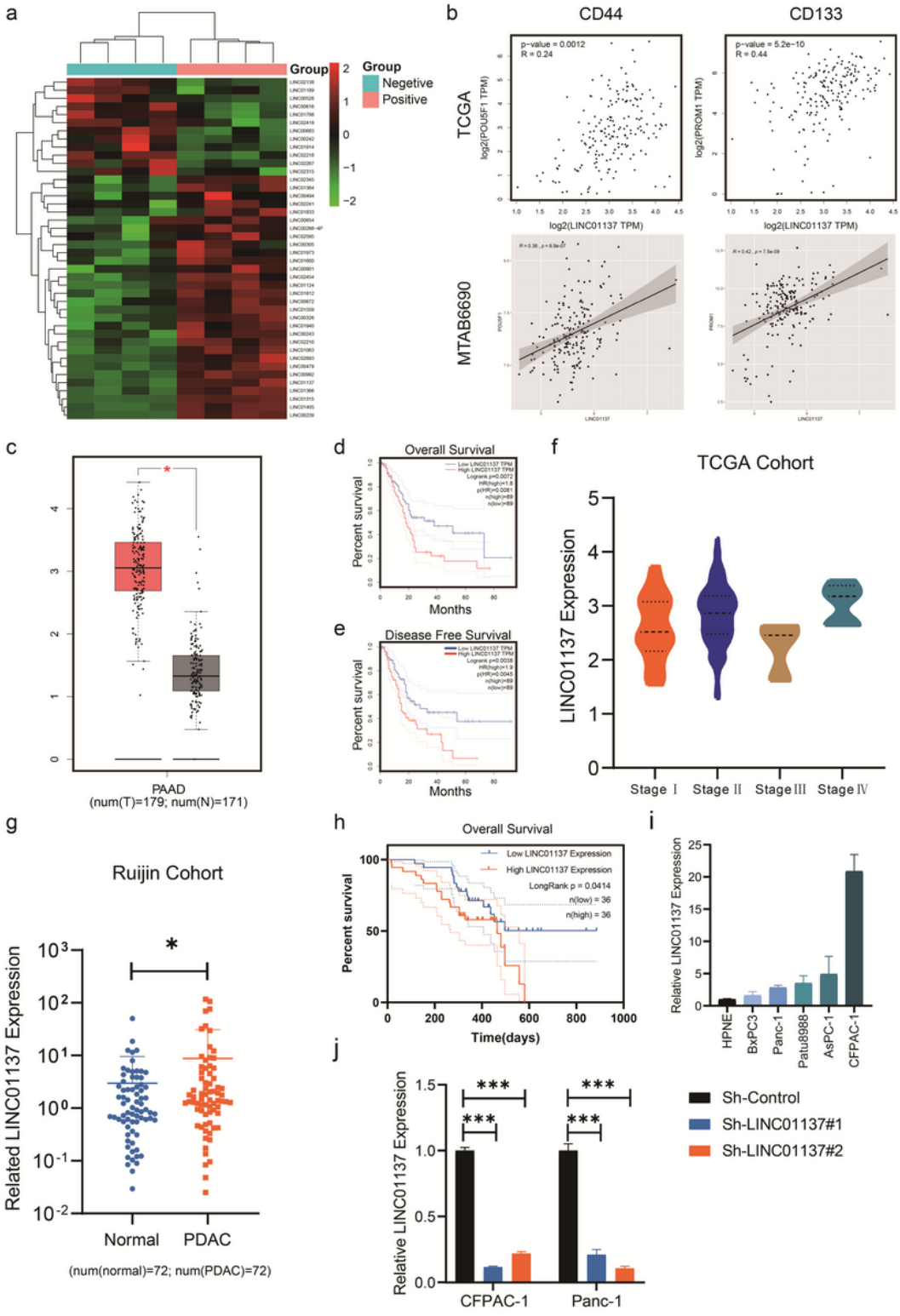

Figure 1

Higher LINC01137 expression in PCSCs was associated with poor outcome. a Heatmap showing the differential long intergenic lncRNAs between CSC-like and non-CSC-like cells whose data was obtained from GSE51971. **b** Relationship between LINC01137 and stemness-associated genes (CD44 and CD133) in TCGA and MTAB 6690. **c** Differential and **d-e** prognostic analyses of LINC01137 in the GEPIA database using data from TCGA. **f** The expression of LINC01137 in patients divided by cancer stages using

expression data from TCGA database (n=179). **g** LINC01137 expression in 72 pairs of PDAC tumor tissues and adjacent normal tissues. **h** Prognostic analysis of LINC01137 using clinical prognostic data of 72 patients from Ruijin Hospital, Shanghai. **i** LINC01137 expression in pancreatic cell lines. **j** Knockdown efficiency of LINC01137 in two pancreatic cell lines (CFPAC-1 and Panc-1). Data are represented as means ± SD.*p<0.05, ***p<0.001.

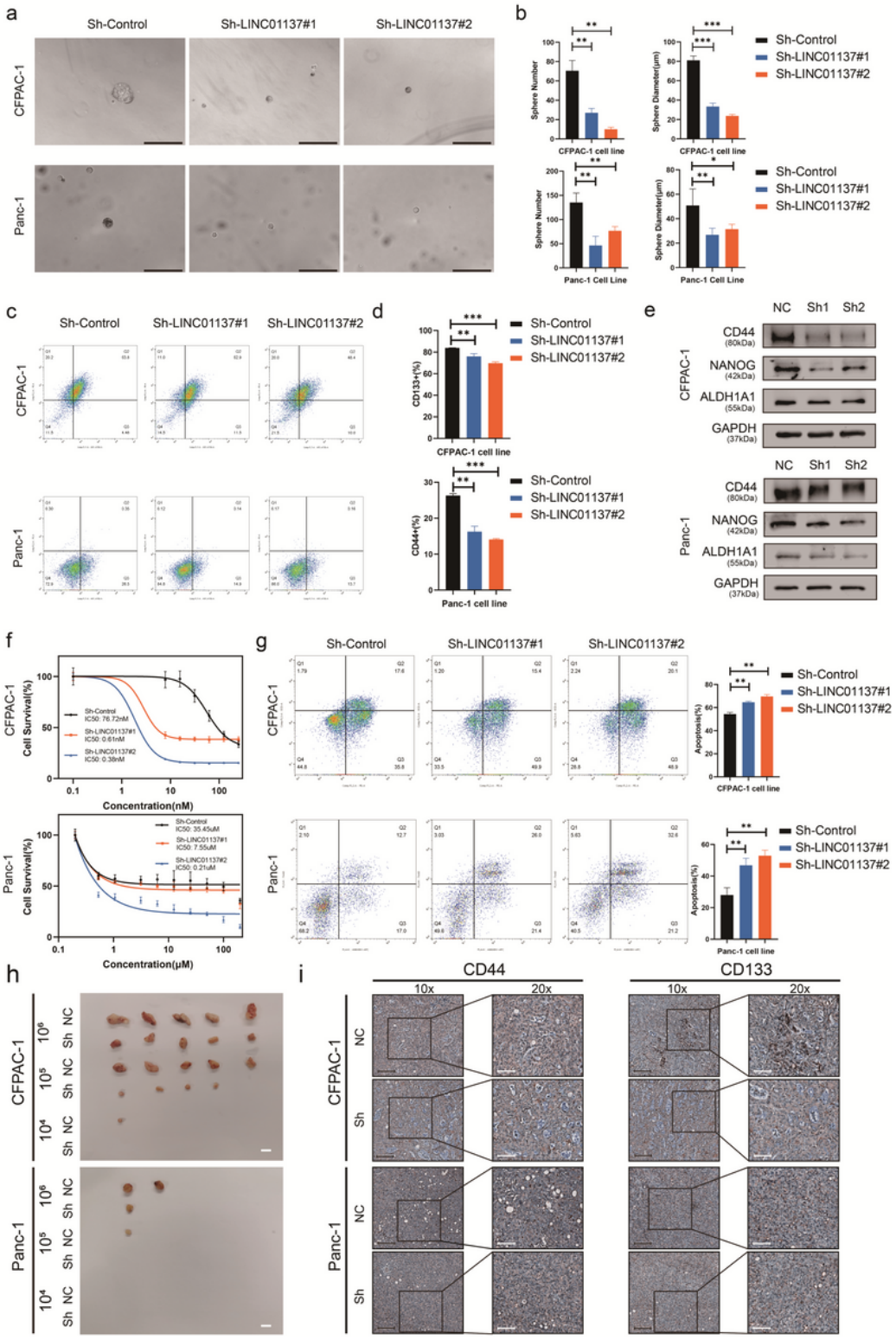

Figure 2

LINC01137 promoted PDAC stemness and gemcitabine chemoresistance. Stemness was verified *in vitro* through **a-b** a sphere formation assay, **c-d** FCM for surface markers and **e** stemness-associated gene expression. **h** Limiting dilution assays of the knockdown group with the negative control group in the CFPAC-1 and Panc-1 cell lines *in vivo*. **i** Immunohistochemistry analysis using sliced tumor tissues derived from CFPAC-1 and Panc-1 cells incubated with CD44 and CD133 antibodies. **f** Gemcitabine inhibitor ratio assay in pancreatic cell lines. **g** Gemcitabine-induced apoptosis tested by FCM. Data are represented as means ± SD. *p<0.05, **p<0.01, ***p<0.001. Black bar, 200 μm. White bar, 1 cm. Black bae with arrows, 200 μm. White bar with arrows, 100 μm.

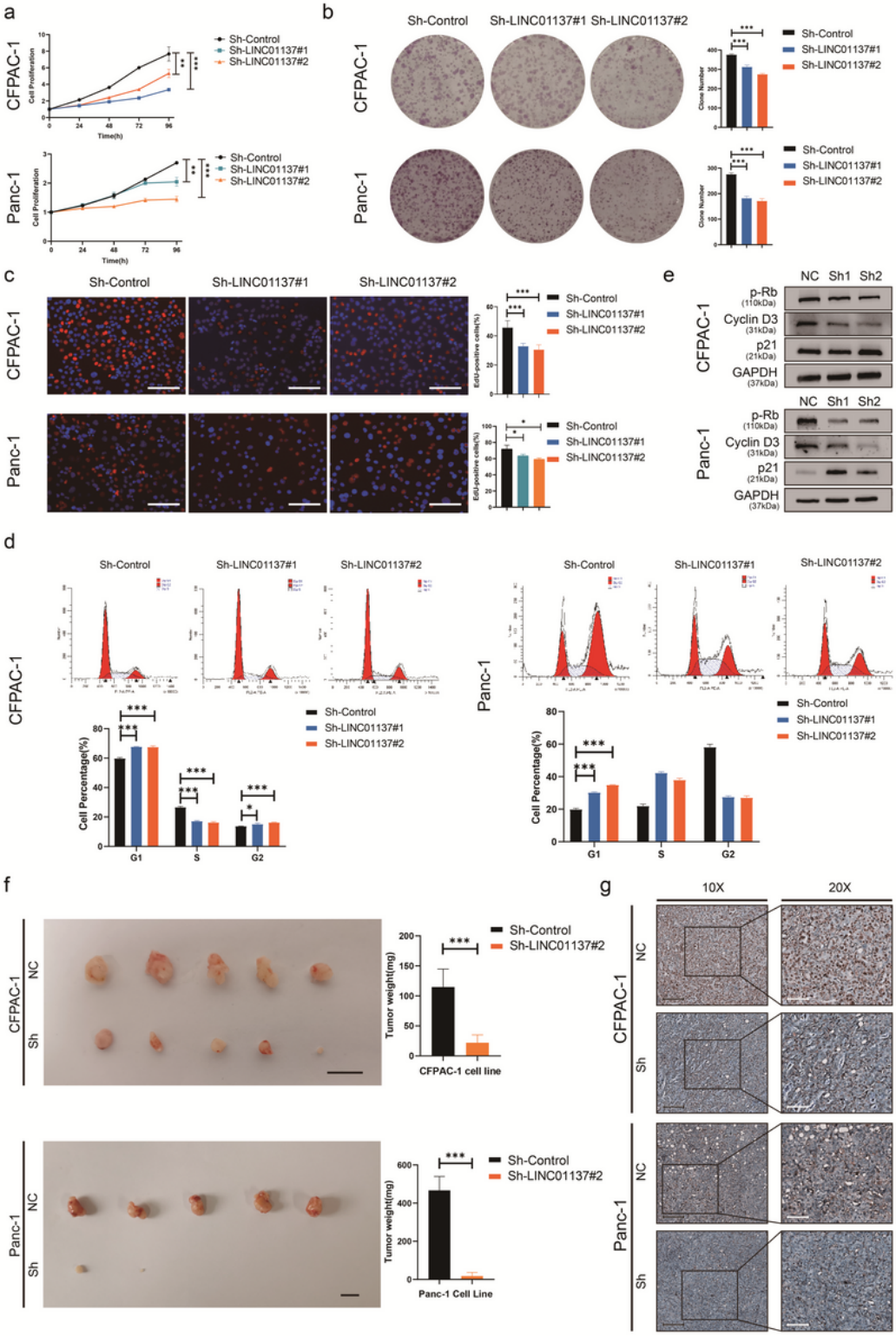

Figure 3

LINC01137 promoted PDAC proliferation and cell cycle. Cell proliferation was illuminated using the **a** CCK-8, **b** colony formation, and **c** EdU assays. **d** Cell cycle assay and G1/S check point strength were verified through FCM. **e** Cell cycle proteins expression. **f** Reduction of pancreatic cancer growth by downgraded LINC01137 expression *in vivo*. **g** Immunohistochemistry staining of xenografts from

different treatment groups. Data are represented as means ± SD. *p<0.05, **p<0.01, ***p<0.001. White bar, 200 μm. Black bar, 1 cm. Black bae with arrows, 200 μm. White bar with arrows, 100 μm.

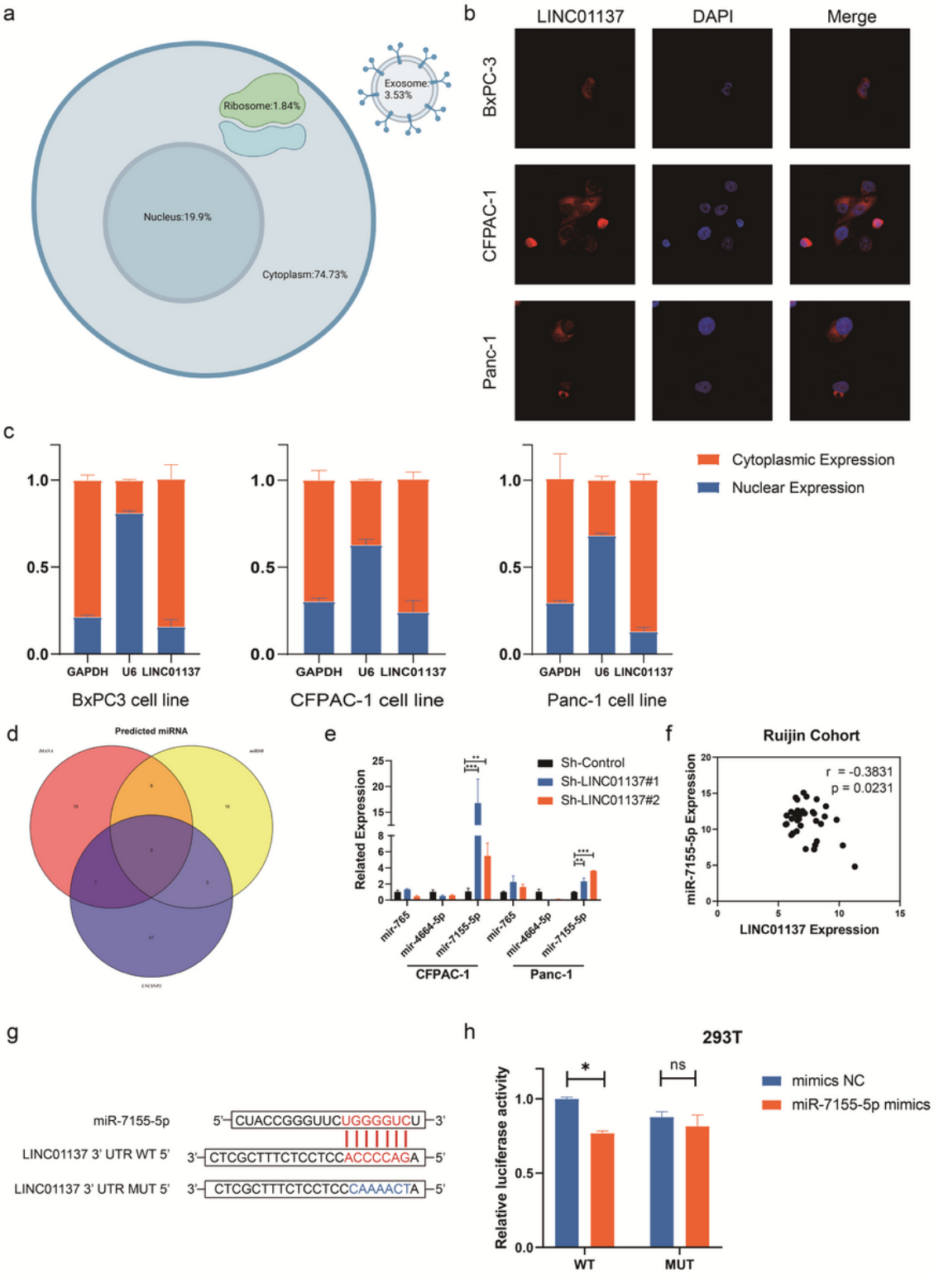

Figure 4

LINC01137 as a competing endogenous RNA (ceRNA) targeted miR-7155-5p. a Potential subcellular location of LINC01137 predicted by lncLocator. **b** FISH for LINC01137 in three pancreatic cancer cell lines (BxPC-3, CFPAC-1, and Panc-1). **c** Subcellular LINC01137 expression verified using nucleocytoplasmic separation; U6 and GAPDH were used for quality control. **d** MiRNAs binding to LINC01137 were predicted using three online databases (DIANA, miRDB, and LNCSNP2). **e** Predicted miRNA expression in the CFPAC-1 and Panc-1 cell lines in the knockdown and control groups. **f** The correlation between LINC01137 and miR-7155-5p expression in 35 PC tumor tissues. **g** WT and MUT LINC01137 3'-UTR report vector construction. **h** Dual-luciferase reporter assay showed that miR-7155-5p overexpression significantly suppressed the activity of the reporter containing WT LINC01137. Data are represented as means ± SD. *p<0.05, **p<0.01, ***p<0.001.

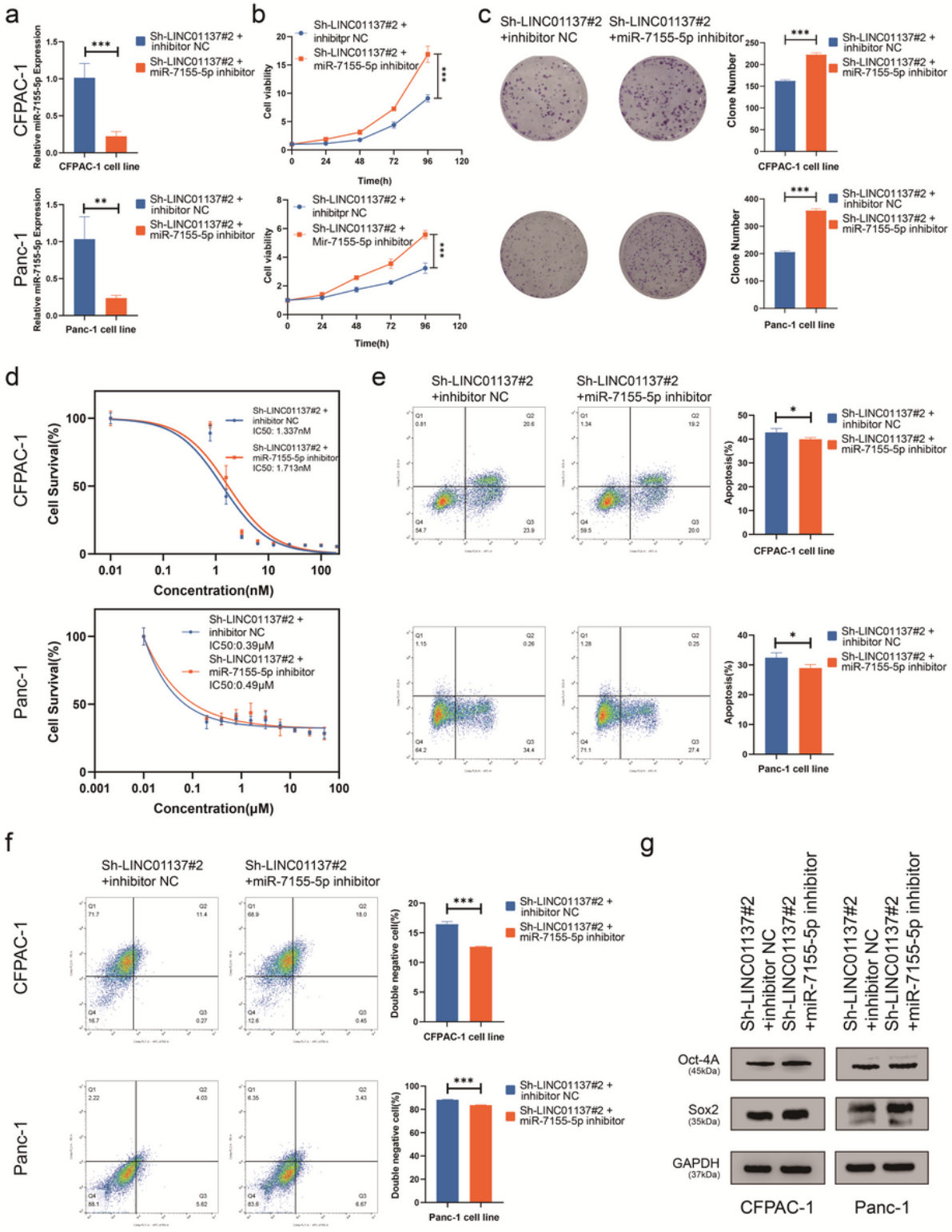

Figure 5

MiR-7155-5p knockdown offset effect of LINC01137 knockdown in PDAC. a Real-time PCR analysis of miR-7155-5p levels in the knockdown group with CFPAC-1 and Panc-1 cells transfected with a negative control inhibitor (inhibitor NC) or a miR-7155-5p inhibitor. Cell growth was verified using **b** CCK-8 and **c** colony formation. Chemoresistance capacity was tested through **d** the gemcitabine inhabitation ratio and

e FCM. Stemness was illuminated through **f** surface marker assay using FCM and **g** the expression of stemness-associated proteins. Data are represented as means ± SD. *p<0.05, **p<0.01, ***p<0.001.

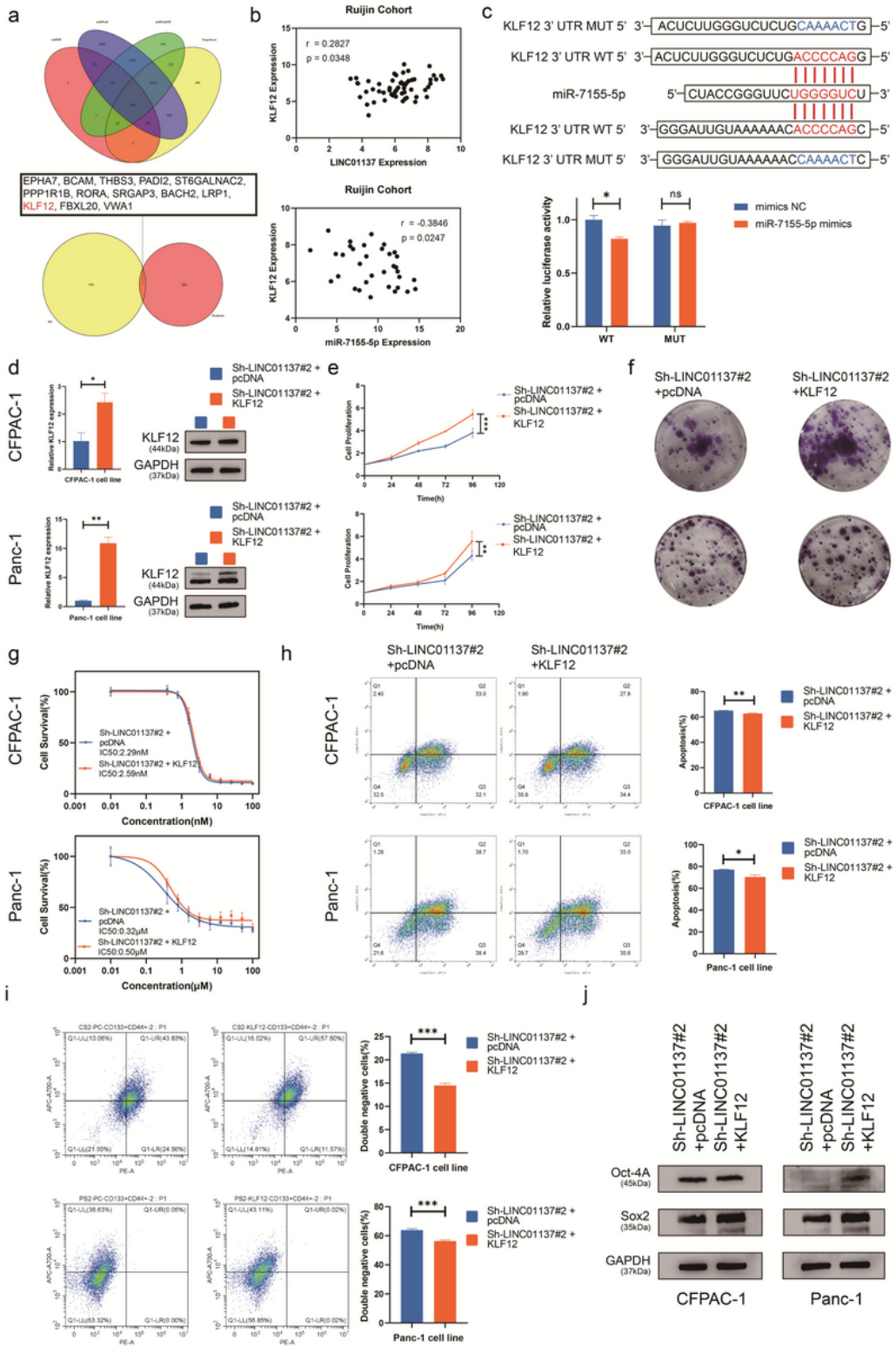

Figure 6

LINC01137 regulated KLF12 through miR-7155-5p. a Upper picture was predicted mRNAs binding to miR-7155-5p in four online datasets (miRDB, miRWalk, miRPathDB, and TargetScan), and under picture was

screened mRNAs selected though combining online datasets results and RNA sequencing results. **b** The correlation between LINC01137 and KLF12 expression in 56 PDAC tumor tissues and the correlation between miR-7155-5p and KLF12 expression in 34 PDAC tumor tissues. **c** Upper section was WT and MUT KLF12 3'-UTR report vector construction, and under section was dual-luciferase reporter assay showed that miR-7155-5p overexpression significantly suppressed the activity of the reporter containing WT KLF12. **d** Real-time PCR analysis and western blotting analysis of KLF12 expression levels in the knockdown group with CFPAC-1 and Panc-1 cells transfected with a negative control vector or a KLF12 cDNA. Cell growth was illuminated using **e** CCK-8 and **f** colony formation. Chemoresistance capacity was verified through **g** the gemcitabine inhabitation ratio and **h** FCM. Stemness was verified through **i** surface marker assay using FCM and **j** the expression of stemness-associated proteins. Data are represented as means ± SD. *p<0.05, **p<0.01, ***p<0.001.

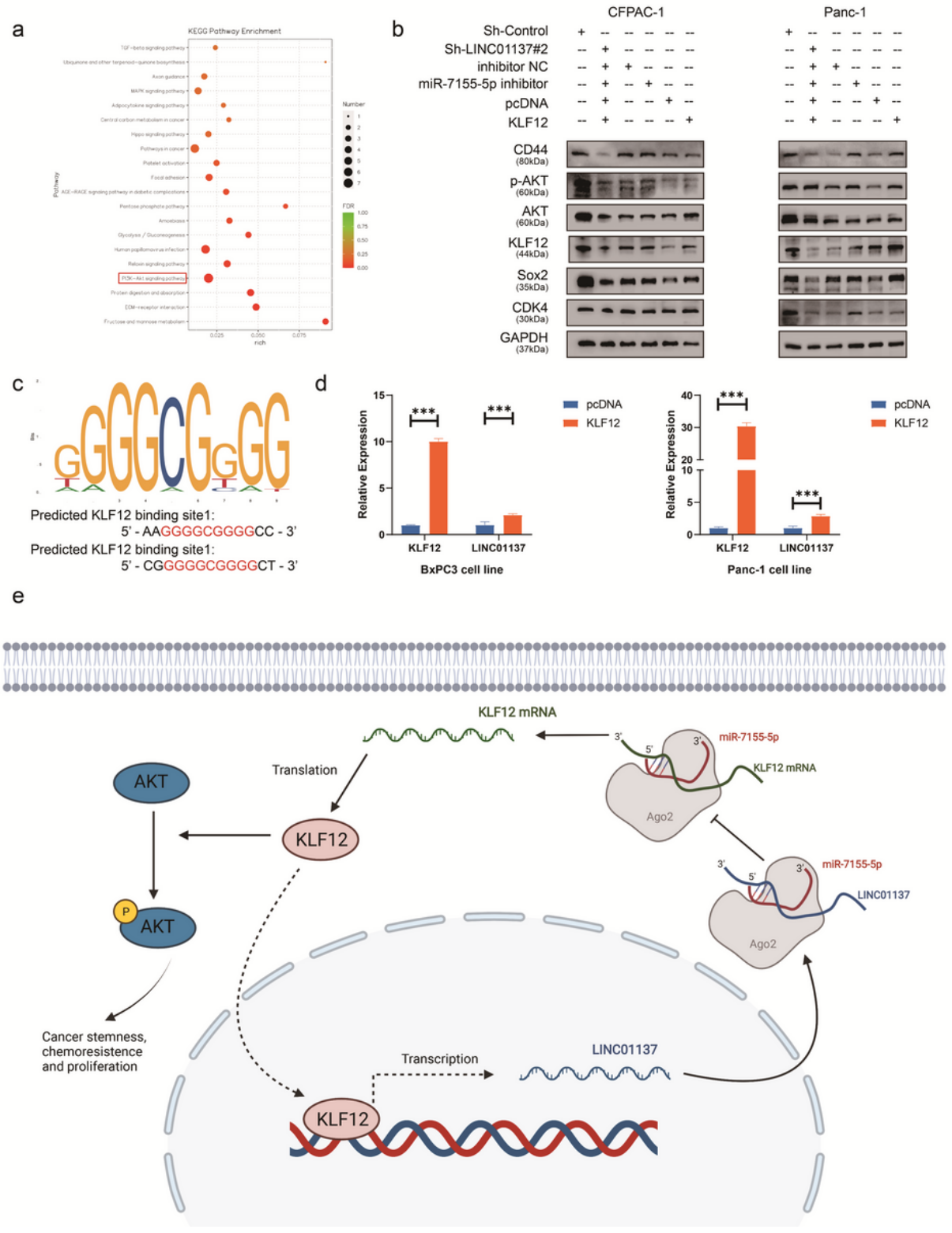

Figure 7

LINC01137 participated in the PI3K/Akt pathway to promote PDAC tumorigenesis through regulating KLF12. a KEGG pathway enrichment between LINC01137 overexpression group and LINC01137 knockdown group in Panc-1 cell line. **b** CD44, p-AKT, AKT, KLF12, Sox2 and CDK4 protein level was detected by western blotting analysis in two pancreatic cancer cell lines (CFPAC-1 and Panc-1) with different treatments. **c** The KLF12 binding motif and possible binding site of KLF12 with LINC01137

provided by the JASPAR database. **d** Real-time PCR analysis of KLF12 and LINC01137 levels in two pancreatic cancer cell lines (BxPC3 and Panc-1) transfected with a negative control pcDNA (pcDNA) or a KLF12 cDNA. **e** Schematic diagram showing the mechanism of how LINC01137 regulates PDAC stemness, chemoresistance and proliferation. Data are represented as means ± SD. *p<0.05, ***p<0.001.

Supplementary Files

This is a list of supplementary files associated with this preprint. Click to download.

- supplementalfigure.pdf